Letters

A 5.8-GHz High-Power and High-Efficiency Rectifier Circuit With Lateral GaN Schottky Diode for Wireless Power Transfer

Kui Dang, Jincheng Zhang, *Member, IEEE*, Hong Zhou, *Member, IEEE*, Sen Huang, Tao Zhang, Zhaoke Bian, Yachao Zhang, Xinhua Wang, Shenglei Zhao, Ke Wei, and Yue Hao, *Senior Member, IEEE*

***Abstract*—In this letter, we propose to implement a microwave lateral GaN Schottky barrier diode (SBD) in a designed 5.8-GHz rectifier circuit for future high-power and high-efficiency wireless power transfer. The low-pressure chemical vapor deposition SiN-passivated lateral GaN SBD demonstrates a low turn-ON voltage of 0.38 V, a low ON-resistance of 4.5 Ω, a low junction capacitance of 0.32 pF at 0-V bias, and a high breakdown voltage of 164 V, which are essentials for a high-efficiency and high-power rectifying application. By incorporating this lateral GaN SBD in a well-designed 5.8-GHz rectifier circuit, an unprecedented combination of high efficiency and high power is achieved simultaneously. The rectifier circuit demonstrates a high RF/dc conversion efficiency ($\eta_{\mathrm{RF/DC}}$) of 71 ± 4.5% with an input power (P_{in}) of 2.5 W and $\eta_{\mathrm{RF/DC}}$ = 50 ± 4.5% with P_{in} = 6.4 W per single diode, showing the great promise of embracing lateral GaN SBD for future wireless high-power transfer application.**

***Index Terms*—Lateral GaN Schottky barrier diode (SBD), rectifier circuit, wireless power transfer (WPT).**

I. Introduction

THE wireless power transfer (WPT) concept was first proposed by Tesla more than 100 years ago, and the WPT has aroused much more interests due to the increased demand of various power supply routes, whereas the conventional wired power transfer is inconvenient or even impossible under some circumstances, such as moving electrical vehicles, unmanned aerial vehicles, solar-powered satellites, implantable medical devices inside the human body, and sending energy to inaccessible buildings or places after severe disasters like earthquake [1]–[8]. The modern era of a microwave WPT system emerged at early 1960s, consisting of large signal generation, transmitting and receiving antennas, rectifier circuit, and output resistive loads. In order to increase the transmission distance, decrease the rectenna aperture size, and minimize the high-frequency microwave power generation cost, the next higher industrial, scientific, and medical band of 5.8 GHz was concentrated [9]. This particular frequency is attractive for beamed power transmission due to its smaller component sizes and a greater transmission range over the 2.45-GHz frequency.

A crucial factor of determining the efficiency of the WPT system is the SBD in the rectifying circuit, which converts the received RF signal into dc power. In order to increase the rectified power and efficiency, the SBD should substantially possess a low turn-ON voltage (V_{on}), a low junction capacitance (C_j), a low on-resistance (R_{on}), and a high breakdown voltage (BV) [10]. However, due to the fundamental and inherent limitations of those parameters, like low V_{on}, low R_{on}, and high BV, it is a challenge for a diode to achieve high efficiency and high power simultaneously. For example, a 5.8-GHz rectifier circuit with commercially available Si or GaAs SBDs can achieve an efficiency of as high as 82%, but the rectified power is just around 40 mW [9]. Therefore, it is desired that the SBD should possess those parameters as ideal as possible so as to embrace the high efficiency and high power at the same time.

On the other hand, two-dimensional electron gas (2DEG) on the GaN-based heterojunction structure has the advantage of high breakdown field and high electron density, mobility, and saturation velocity; therefore, low R_{on}, high BV, and low C_j can be achieved [11]. By engineering the anode region with low work-function metal and enhanced surface passivation, extremely low V_{on} and high BV can be satisfied. In this letter, for the first time, we propose to incorporate a high-performance lateral GaN diode into a well-designed 5.8-GHz rectifier circuit, and a high RF/dc conversion efficiency ($\eta_{\mathrm{RF/DC}}$) of 71 ± 4.5% with an input power (P_{in}) of 2.5 W and $\eta_{\mathrm{RF/DC}}$ = 50 ± 4.5% with P_{in} = 6.4 W per single diode are demonstrated, showing a significant progress achieved in the WPT system at 5.8 GHz.

Manuscript received July 2, 2019; revised August 7, 2019; accepted August 22, 2019. Date of publication August 29, 2019; date of current version December 13, 2019. This work was supported in part by the National Key Research and Development Program under Grant 2016YFB0400100, in part by the National Key Science and Technology Special Project under Grant 2017ZX01001301, in part by the National Natural Science Foundation of China under Grants 11435010 and 61474086, in part by the Natural Science Basic Research Program of Shaanxi under Grant 2016ZDJC-02, and in part by the State Key Laboratory on Integrated Optoelectronics under Grant IOSKL2018KF04. *(Corresponding authors: Jincheng Zhang; Hong Zhou.)*

K. Dang, J. Zhang, H. Zhou, T. Zhang, Z. Bian, Y. Zhang, S. Zhao, and Y. Hao are with the Key Laboratory of Wide Band Gap Semiconductor Materials and Devices, School of Microelectronics, Xidian University, Xi'an 710071, China (e-mail: dangkui@vip.qq.com; jchzhang@xidian.edu.cn; hongzhou@xidian.edu.cn; zhangtao9204@sina.com; zkbian@stu.xidian.edu.cn; ychzhang@xidian.edu.cn; slzhao@xidian.edu.cn; yhao@xidian.edu.cn).

S. Huang, X. Wang, and K. Wei are with the Institute of Microelectronics of Chinese Academy of Sciences, Beijing 100029, China (e-mail: huangsen@ime.ac.cn; wangxinhua@ime.ac.cn; weike@ime.ac.cn).

Color versions of one or more of the figures in this article are available online at http://ieeexplore.ieee.org.

Digital Object Identifier 10.1109/TPEL.2019.2938769

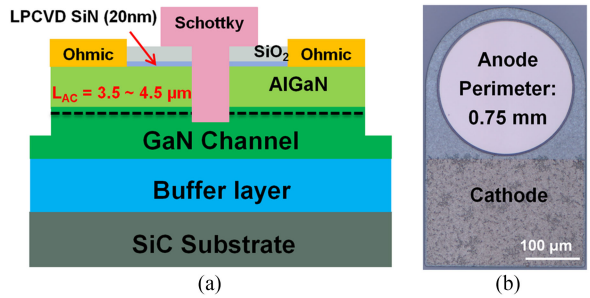

Fig. 1. (a) Cross-sectional schematic view of the lateral GaN-on-SiC SBD. (b) Microscopy image of the fabricated lateral GaN SBD.

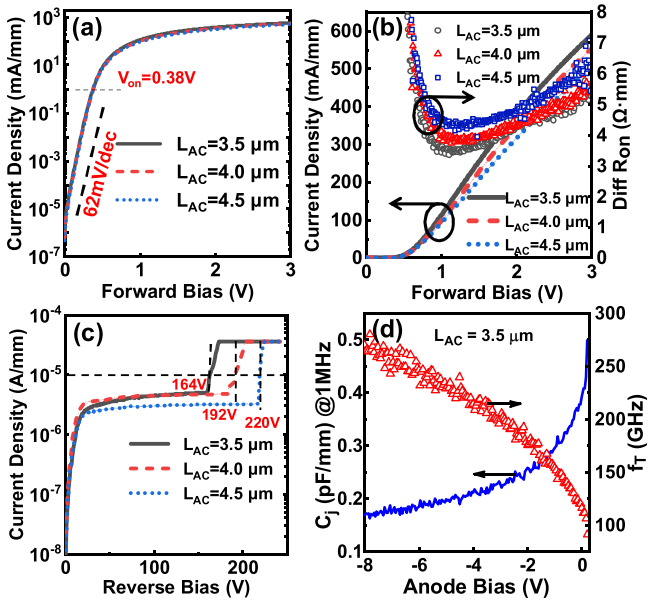

Fig. 2. Forward *I–V* characteristics at room temperature in (a) log-scale and (b) linear-scale plots of the fabricated lateral GaN-on-SiC SBDs. (c) Room temperature reverse *I–V* performance of GaN SBDs with various $L_{\rm AC}$s. (d) Room temperature C_j and f_T versus anode bias characteristics of the lateral GaN SBD. Low $V_{\rm on} = 0.38$ V, low $R_{\rm on} = 4.5\ \Omega$, high BV = 164 V, high $f_T = 111$ GHz, and low $C_j = 0.32$ pF are achieved.

II. GaN Diode Fundamentals

Fig. 1 shows the cross-sectional schematic and fabricated circular-shaped lateral GaN SBDs on the SiC substrate. Lateral GaN SBDs are commenced with depositing a 20 nm of low-pressure chemical vapor deposition (LPCVD) passivation layer on the epitaxial wafer surface, which is a core technique to suppress the power loss and $\eta_{\rm RF/DC}$ degradation when the diode is switching between high reverse and forward biases. Other advanced technologies, including low damage etching and anode engineering, have all been implemented to make the GaN SBD as ideal as possible. More details about the SBD fabrications can be found in our previous work [10].

Fig. 2(a) shows the well-behaved log-scale forward *I–V* characteristics of the lateral GaN SBD. An extremely low $V_{\rm on} = 0.38$ V and near ideal subthreshold swing of 62 mV/dec are achieved, verifying that the GaN SBD is approaching its ideal situation due to the engineered process. The linear-scale forward *I–V* and $R_{\rm on}$–*V* are depicted in Fig. 2(b). The $R_{\rm on}$ of the GaN SBD with 0.75-mm perimeter is extracted to be 4.5 Ω at an anode–cathode distance ($L_{\rm AC}$) of 3.5 μm. The reverse *I–V* performances of the GaN SBDs are displayed in Fig. 2(c). A high BV of 164 V is acquired, which is several times higher than that of Si and GaAs SBDs at a similar $R_{\rm on}$ and C_j, indicating a much higher $P_{\rm in}$ can be rectified. The C_j and cutoff frequency (f_T) behaviors are summarized in Fig. 2(d). A low $C_j = 0.32$ pF is measured at bias of 0 V, yielding a high $f_T = 111$ GHz, considering the equation $f_T = 1/(2 \times \pi \times R_{\rm on} \times C_j)$. More analysis and device physics are beyond the scope of this letter, and they can be found on our other works [10].

In order to maintain a high efficiency under high $P_{\rm in}$ condition, the current collapse phenomenon should be minimized, which is defined as the rectified current or $R_{\rm on}$ degradation when the diode is switching between high reverse and forward biases. The dynamic $R_{\rm on}$ degradation effect will be more pronounced under higher reverse biases so that the $\eta_{\rm RF/DC}$ will be more compromised at higher $P_{\rm in}$ and higher frequency. This phenomenon is related to the diode surface passivation. Therefore, the diode should be carefully designed to avoid the power-loss-induced $\eta_{\rm RF/DC}$ decrease. The dynamic behaviors of our fabricated GaN SBD on the SiC substrate with state-of-the-art LPCVD SiN and atomic layer deposition (ALD) Al_2O_3 passivation are compared in Fig. 3(a) and (b), respectively. To mimic the rectifying process at different $P_{\rm in}$, various reverse anode biases as the stress base are imposed on the SBD for different durations, and then, the anode bias is switched to positive forward values from 0 to 1.5 V to turn ON the device. The dynamic differential $R_{\rm ON}$ is extracted from the linear region of the forward *I–V*. For example, stress bases start from −20 to −100 V with −20 V as the step, and stress times from 1 ms to 10 s with one decade as the duration were adopted. It is obvious that with the LPCVD SiN passivation, the GaN SBD undergoes a negligible current collapse even at high stress base and long duration. Fig. 3(c) shows the extracted dynamic $R_{\rm ON}$ degradation percentage at different stress bases and times. The dynamic $R_{\rm ON}$ at a −100 V reserve stress voltage and 10 s duration is just 1.08 times when compared with the one with ALD passivation (1.35 times) under the same measurement setup, indicating a lower power loss and higher $\eta_{\rm RF/DC}$ under the higher $P_{\rm in}$ circumstance.

The current collapse mechanism due to the unoptimized surface passivation is shown in Fig. 4(a) and (b). When the anode is reversely biased, electrons from the anode and 2DEG channel are captured by the unpassivated surface states at the top of the AlGaN barrier, such that the surface is negatively charged. Those negative charges deplete the 2DEG channel leading to the reduced 2DEG density ($n_{\rm 2DEG}$). Therefore, the resistance of the GaN SBD is increased, resulting in a reduced efficiency. For this particular case, with the state-of-the-art passivation technique by LPCVD SiN, the surface state is reduced so that the current collapse phenomenon is negligible when compared with the ALD Al_2O_3 surface passivation.

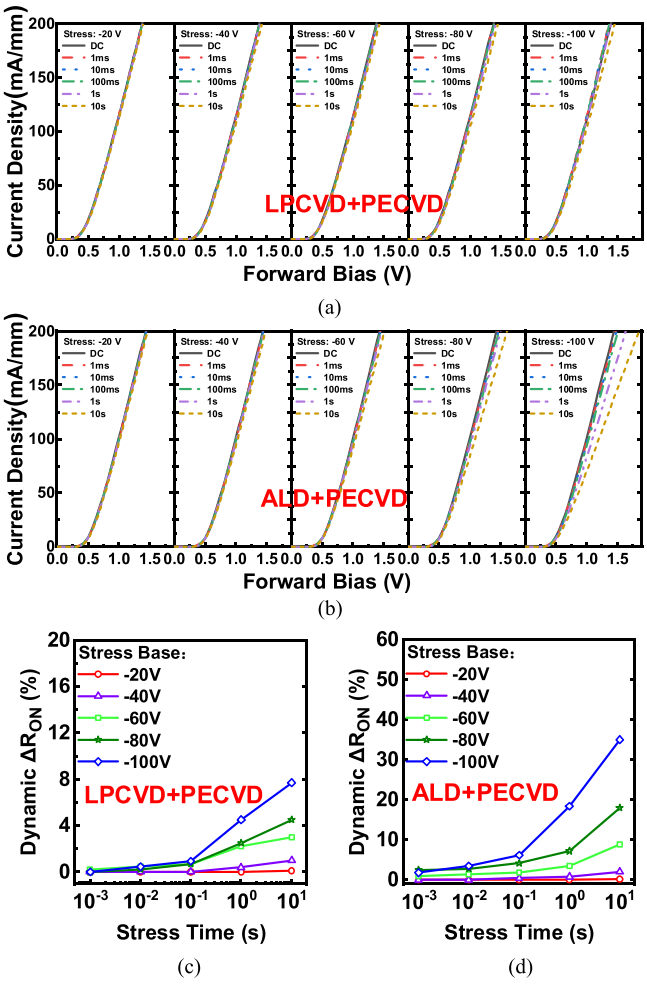

Fig. 3. Linear-scale forward *I–V* characteristics of the lateral GaN SBD with (a) LPCVD + PECVD and (b) ALD + PECVD passivation at stress bases of −20, −40, −60, −80, and −100 V and stress time of 10^{-3}, 10^{-2}, 10^{-1}, 1, and 10 s, respectively. Extracted dynamic ΔR_{on}–stress time at various stress bases and times of the lateral GaN SBD with (c) LPCVD + PECVD and (d) ALD + PECVD passivations. Negligible dynamic R_{on} degradation is observed for LPCVD + PECVD passivation.

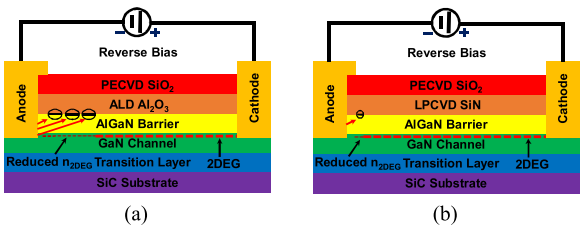

Fig. 4. (a) ALD Al_2O_3 and (b) LPCVD SiN with PECVD SiO_2 surface passivation influences on the 2DEG channel of the lateral GaN SBD when the diode is reversely biased. With the LPCVD SiN passivation, the surface state is suppressed so that the current collapse is mitigated.

III. Rectifier Circuit With the Lateral GaN SBD

A. Rectifier Circuit Design

The schematic of the rectifier circuit is shown in Fig. 5(a). Advanced design system (ADS) by Keysight Technology was utilized for the rectifier circuit design and simulation. The designed layout is exported to the computer-aided design and then prototyped with the Rogers5880 substrate. The manufactured circuit and packaged GaN SBD are shown in Fig. 5(b). The similar RF/dc conversion efficiency measurement and how RF input power is determined can be found in [14]. A Murata ceramic capacitor with a capacitance of 4.3 pF is used in the RF/dc conversion measurement to prevent the dc power feeding back. A lateral GaN SBD model is designed and implemented during the rectifier circuit design. The rectifier circuit is designed and optimized for the 5.8-GHz microwave rectification, and a three-open-stub HF filter before the GaN SBD is implemented to suppress its second, third, and fourth harmonics for this 5.8-GHz signal, while this 5.8-GHz signal is allowed to pass through. Another three-open-stub dc filter after the GaN SBD is used to suppress its second and third harmonics for this 5.8-GHz signal. ADS S_{21} simulation was performed to confirm the filter design, as shown in Fig. 6(a).

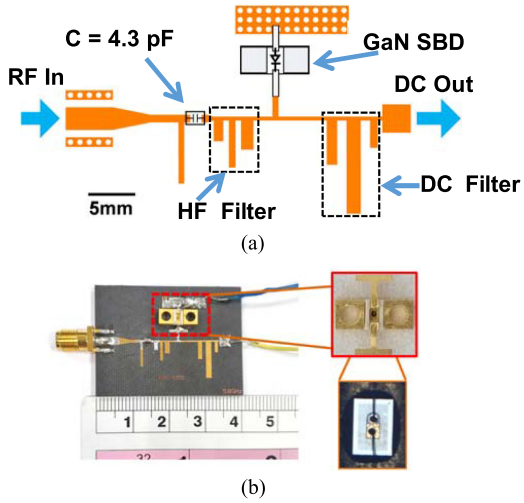

Fig. 5. (a) Schematic of a 5.8-GHz microwave rectifier with designed harmonic suppression structure. (b) Photography of the manufactured rectifier circuit and packaged lateral GaN SBD.

Unlike the previous rectifier circuit designed for small input power (10–20 dBm) at 5.8 GHz, this circuit needs to accommodate high power (>30 dBm), which suffers from more severe nonlinearity induced impedance mismatching and cause power loss. The simulated S_{11} of the rectifier circuit versus input power are depicted in Fig. 6(b). The circuit is designed to suppress the reflection and provide better matching at higher input power levels from 30 to 40 dBm to achieve a higher conversion efficiency. The input impedance Z_L of the rectifier varies from (56.6−j106.3) to (37.9−j32.8) Ω when the input power ranges from 10 to 45 dBm, as shown in Fig. 6(c). The impedance (54.7–j1.6) Ω at an input power of 38–39 dBm is chosen as the reference impedance to ensure the low reflection and high efficiency at the high P_{in}. The simulated and measured conversion efficiencies versus input power are depicted in Fig. 6(d). The measured results agree quite well with the simulated ones at the P_{in} range of 10–35 dBm. The difference between the

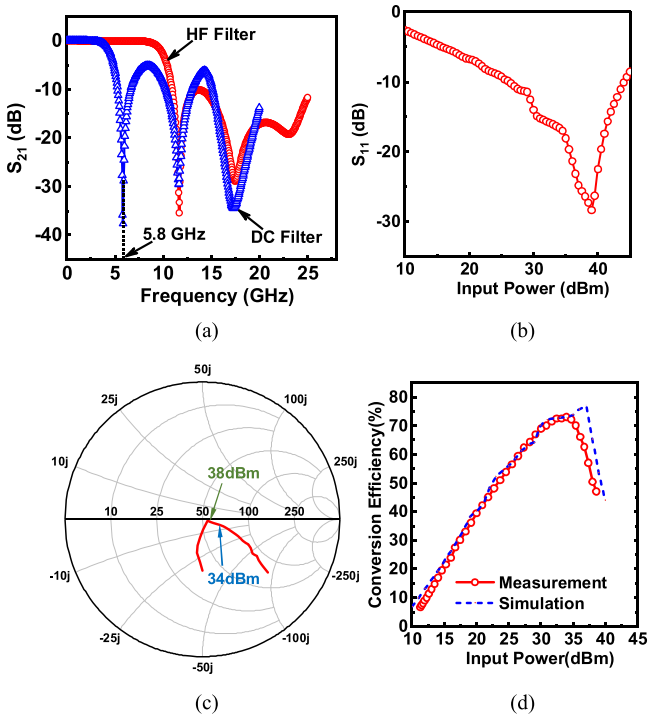

Fig. 6. (a) Simulated S_{21} of a high-frequency filter with suppressed second, third, and fourth harmonics and a dc pass filter with a suppressed 5.8-GHz signal and second and third harmonics. (b) Simulated circuit S_{11} versus input power to show the suppressed reflection at high input power of 30–40 dBm. (c) Input impedance of the designed rectifier circuit with $P_{\rm in}$ from 10 to 45 dBm. (d) Measured and simulated efficiencies of the rectifier circuit with the lateral GaN SBD at 5.8 GHz.

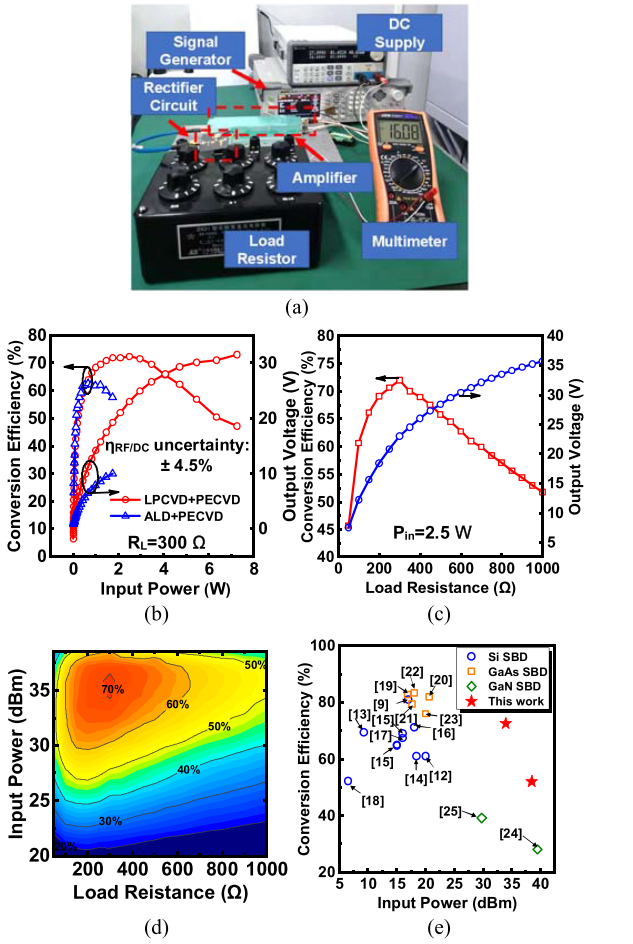

Fig. 7. (a) Prototype of the 5.8-GHz rectifier circuit experimental test setup. Conversion efficiency and output voltage dependence of the (b) input power and (c) load resistance of the lateral GaN SBD with peak $\eta_{\rm RF/DC} = 71 \pm 4.5\%$ at $P_{\rm in} =$ of 2.5 W and $\eta_{\rm RF/DC} = 50 \pm 4.5\%$ at $P_{\rm in} =$ of 6.4 W. (d) Conversion efficiency versus input power and load resistance at frequency of 5.8 GHz. (e) Conversion efficiency versus input power of some state-of-the-art rectifier circuit with Si, GaAs, and vertical GaN SBDs. Our lateral GaN SBD presents the best combination of $\eta_{\rm RF/DC}$ and $P_{\rm in}$.

measured and simulated ones at high $P_{\rm in}$ is caused by the diode entering the forward current saturation mode and diode model inaccuracy.

B. Rectifier Circuit Characterization

The rectifier circuit test system is shown in Fig. 7(a), consisting of a 5.8-GHz signal generator RIGOL DSG3060, a GaN high-electron-mobility transistor power amplifier, a dc power supply IVYTECH IPS-600B-30-20, a precision ZX21 resistor box, and a multimeter VICTOR VC890C+. An attenuator HBTE-CA200-8-20-N and an NRP-18S RF power meter from Rohde & Schwarz are also included to calibrate the input and output power of the power amplifier. The overall inaccuracy of the input/output power measurement is determined to be ± 0.194 dB, which is converted to be $\pm 4.5\%$. The $\eta_{\rm RF/DC}$ can be calculated as $\eta_{\rm RF/DC} = P_{\rm DC}/P_{\rm in} = V_{\rm DC}{}^2/(R_L \times P_{\rm in})$, where $V_{\rm DC}$, R_L, $P_{\rm in}$ are output voltage, load resistance, and input power, respectively. Fig. 7(b) presents the $\eta_{\rm RF/DC}$ and output voltage $V_{\rm DC}$ versus $P_{\rm in}$ of the rectifier circuit with lateral GaN SBDs. With the advanced surface passivation technique by combining LPCVD and plasma-enhanced chemical vapor deposition (PECVD) processes, the lateral GaN SBD demonstrates a peak efficiency of $71 \pm 4.5\%$. As a contrast, the one with ALD and PECVD passivation shows a similar $\eta_{\rm RF/DC}$ at low $P_{\rm in}$; however, the $\eta_{\rm RF/DC}$ only reaches 63% and, then start to drop rapidly due to the dynamic $R_{\rm on}$ increases dramatically at the higher $P_{\rm in}$, which is in coincidence with our dynamic $R_{\rm on}$ characterization. The peak $\eta_{\rm RF/DC} = 71 \pm 4.5\%$ is achieved at a $P_{\rm in} = 2.5$ W and R_L of 300 Ω. Meanwhile, the rectifier circuit also achieves a $\eta_{\rm RF/DC} = 50 \pm 4.5\%$ at a $P_{\rm in} = 6.4$ W, indicating a significant progress of the $P_{\rm in}$ when compared with the Si and GaAs SBD at the same 50% efficiency. Fig. 7(c) depicts the $\eta_{\rm RF/DC}$ and $V_{\rm DC}$ dependence of the R_L at $P_{\rm in} = 2.5$ W and $f = 5.8$ GHz. Fig. 7(d) shows the $\eta_{\rm RF/DC}$ dependence on the $P_{\rm in}$ and R_L at $f = 5.8$ GHz. The $\eta_{\rm RF/DC}$ remains to be higher than $50 \pm 4.5\%$ from the R_L of more than 100 Ω and $P_{\rm in}$ from 27 to 39 dBm, verifying the designed rectifier circuit can accommodate very high power and large range of the R_L. The performance of our rectifier circuit with the lateral GaN SBD are benchmarked against some state-of-the-art rectifier circuit with Si, GaAs or even vertical GaN SBD in the plot of $\eta_{\rm RF/DC}$ versus $P_{\rm in}$ in Fig. 7(e) [9], [12]–[25]. Compared with Si or GaAs SBD, our lateral GaN SBD can provide a similar or slightly lower peak

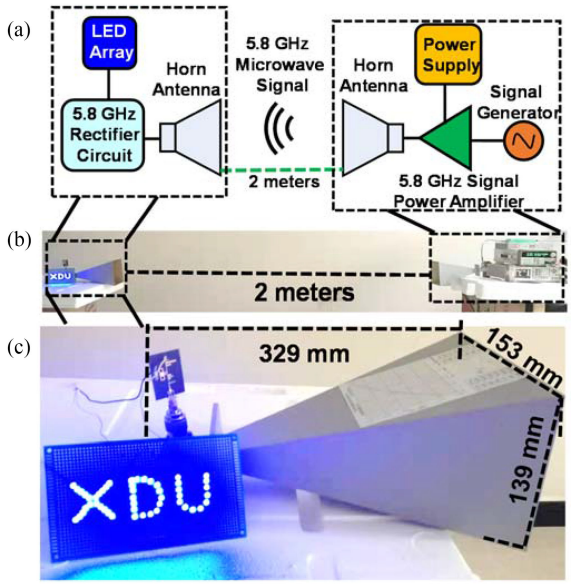

Fig. 8. (a) Schematic of the WPT system. (b) Prototype of the WPT system. (c) Zoomed-in view of the receiving horn antenna with dimension marked and the lighted LED.

$\eta_{\mathrm{RF/DC}}$; however, the rectified power can be 20 times higher. The slightly lower peak efficiency of our lateral GaN SBD is due to the self-heating-effect-induced raised diode temperature and resistance when the diode is rectifying several Watt power and also the parasitic overlap capacitance. Further optimization of the thermal management and adoption of the self-align process to minimize the overlap capacitance can essentially increase the rectifying efficiency. In addition, when compared with the vertical GaN SBD, our lateral GaN SBD can provide almost twice $\eta_{\mathrm{RF/DC}}$ at a similar P_{in}. The vertical GaN SBD even cannot achieve 50% efficiency at all P_{in} ranges, verifying that the lateral GaN SBD is much more suitable for the high-frequency microwave rectifier circuit.

IV. WPT System Demonstration

A microwave WPT system was constructed with the rectifier circuit and designed 5.8-GHz horn antennas. The WPT system block diagram is shown in Fig. 8(a). Two horn antennas with an operating frequency of 5.8 GHz and a standard gain of 20 dBi were designed and manufactured. The spacing between the two 5.8-GHz horn antennas is fixed to be around 2 m, and the two horn antennas are aligned horizontally. The transmitting antenna is connected to an RF power amplifier, a dc power supply, and a 5.8-GHz signal generator, and the receiving antenna supplies received 5.8-GHz RF signal to the rectifier circuit with an SMA connector to light up the LED array with three characters "XDU," as shown in Fig. 8(b). The shape and dimension of the transmitting and receiving horn antennas are depicted in Fig. 8(c). Every five LEDs are connected in series to achieve a total voltage of about 14 V, considering the voltage drop of per single blue LED is about 2.8 V, and then connected in parallel to share the current. The whole WPT efficiency is primarily determined by three aspects, namely the power amplification efficiency (η_1), antenna transmission and receiving efficiency (η_2) at a particular distance of 2 m, and the rectifier circuit efficiency (η_3). The η_1, η_2, and η_3 are determined to be 60%, 4%, and 54%, respectively. Therefore, the overall WPT system has an efficiency $\eta = \eta_1 \times \eta_2 \times \eta_3 = 60\% \times 4\% \times 54\% = 1.3\%$. Further optimizing the power amplifier and antennas can substantially improve the total efficiency of the WPT system.

V. Conclusion

In conclusion, we have demonstrated a state-of-the-art 5.8-GHz microwave rectifier circuit with simultaneously achieving high efficiency and high power for the WPT application. Benefited from the unique property of the GaN, this novel lateral GaN SBD demonstrates low $V_{\mathrm{on}} = 0.38$ V, low $R_{\mathrm{on}} = 4.5\ \Omega$, low $C_j = 0.32$ pF, and high BV = 164 V, which satisfy the fundamental requirements for high-efficiency and high-power microwave rectification. After implementing the high-performance lateral GaN SBD into the optimized and harmonics-suppressed rectifier circuit, high $\eta_{\mathrm{RF/DC}}$ of $71 \pm 4.5\%$ is achieved at a $P_{\mathrm{in}} = 2.5$ W, and $\eta_{\mathrm{RF/DC}}$ of $50 \pm 4.5\%$ is demonstrated at a $P_{\mathrm{in}} = 6.4$ W per single lateral GaN SBD. Compared with the rectifier circuit with Si and GaAs SBDs, our rectifier circuit with the GaN SBD can substantially sustain a $20\times$ higher P_{in}, showing its great potential for future wireless high-power transfer application.

References

[1] M. Cheney, *Tesla Man Out of Time*. Englewood Cliffs, NJ, USA: Prentice-Hall, 1981.
[2] S. Y. R. Hui, W. Zhong, and C. K. Lee, "A critical review of recent progress in mid-range wireless power transfer," *IEEE Trans. Power Electron.*, vol. 29, no. 9, pp. 4500–4511, Sep. 2014.
[3] Z. Zhang, H. Pang, A. Georgiadis, and C. Cecati, "Wireless power transfer—An overview," *IEEE Trans. Ind. Electron.*, vol. 66, no. 2, pp. 1044–1058, Feb. 2019.
[4] Z. Zhang and K. T. Chau, "Homogeneous wireless power transfer for move-and-charge," *IEEE Trans. Power Electron.*, vol. 30, no. 11, pp. 6213–6220, Nov. 2015.
[5] C. Song *et al.*, "Matching network elimination in broadband rectennas for high-efficiency wireless power transfer and energy harvesting," *IEEE Trans. Ind. Electron.*, vol. 64, no. 5, pp. 3950–3961, May 2017.
[6] W. Zhang, J. C. White, A. M. Abraham, and C. C. Mi, "Loosely coupled transformer structure and interoperability study for EV wireless charging systems," *IEEE Trans. Power Electron.*, vol. 30, no. 11, pp. 6356–6367, Nov. 2015.
[7] S. C. Tang, T. L. T. Lun, Z. Guo, K. W. Kwok, and N. J. McDannold, "Intermediate range wireless power transfer with segmented coil transmitters for implantable heart pumps," *IEEE Trans. Power Electron.*, vol. 32, no. 5, pp. 3844–3857, May 2017.
[8] J. Choi, D. Tsukiyama, Y. Tsuruda, and J. M. R. Davila, "High-frequency, high-power resonant inverter with eGaN FET for wireless power transfer," *IEEE Trans. Power Electron.*, vol. 33, no. 3, pp. 1890–1896, Mar. 2018.
[9] J. O. McSpadden, L. Fan, and K. Chang, "Design and experiments of a high-conversion-efficiency 5.8-GHz rectenna," *IEEE Trans. Microw. Theory Techn.*, vol. 46, no. 12, pp. 2053–2060, Dec. 1998.
[10] T. Zhang *et al.*, "1.9 kV/2.61 m$\Omega\cdot$cm^2 lateral GaN Schottky barrier diode on silicon substrate with tungsten anode and low turn-on voltage of 0.35 V," *IEEE Electron Device Lett.*, vol. 39, no. 10, pp. 1548–1551, Oct. 2018.
[11] H. Zhou *et al.*, "High performance InAlN/GaN MOSHEMTs enabled by atomic layer epitaxy MgCaO as gate dielectric," *IEEE Electron Device Lett.*, vol. 37, no. 5, pp. 556–559, May 2016.
[12] B. Zhang, C. Yu, and C. Liu, "Design of a capacitor-less 5.8-GHz microwave rectifier for microwave power transmission," in *Proc. Eur. Microw. Conf.*, 2013, pp. 908–911.

[13] P. Lu, X. Yang, J. Li, and B. Wang, "Polarization reconfigurable broadband rectenna with tunable matching network for microwave power transmission," *IEEE Trans. Antennas Propag.*, vol. 64, no. 3, pp. 1136–1141, Mar. 2016.

[14] Z. Du and X. Y. Zhang, "High-efficiency single- and dual-band rectifiers using a complex impedance compression network for wireless power transfer," *IEEE Trans. Ind. Electron.*, vol. 65, no. 6, pp. 5012–5022, Jun. 2018.

[15] P. Lu, X. Yang, J. Li, and B. Wang, "A compact frequency reconfigurable rectenna for 5.2- and 5.8-GHz wireless power transmission," *IEEE Trans. Power Electron.*, vol. 30, no. 11, pp. 6006–6010, Nov. 2015.

[16] Y. Liu, K. Huang, Y. Yang, and B. Zhang, "A low-profile lightweight circularly polarized rectenna array based on coplanar waveguide," *IEEE Antennas Wireless Propag. Lett.*, vol. 17, no. 9, pp. 1659–1663, Sep. 2018.

[17] Q. Chen, X. Chen, and X. Duan, "Investigation on beam collection efficiency in microwave wireless power transmission," *J. Electromagn. Waves Appl.*, vol. 32, no. 9, pp. 1136–1151, 2018.

[18] P. Lu, K. M. Huang, Y. Yang, F. Cheng, and L. Wu, "Frequency-reconfigurable rectenna with an adaptive matching stub for microwave power transmission," *IEEE Antennas Wireless Propag. Lett.*, vol. 18, no. 5, pp. 956–960, May 2019.

[19] Y.-H. Suh and K. Chang, "A high-efficiency dual-frequency rectenna for 2.45- and 5.8-GHz wireless power transmission," *IEEE Trans. Microw. Theory Techn.*, vol. 50, no. 7, pp. 1784–1789, Jul. 2002.

[20] B. Strassner and Kai Chang, "5.8-GHz circularly polarized dual-rhombic-loop traveling-wave rectifying antenna for low power-density wireless power transmission applications," *IEEE Trans. Microw. Theory Techn.*, vol. 51, no. 5, pp. 1548–1553, May 2003.

[21] J. Guo, H. Zhang, and X. Zhu, "Theoretical analysis of RF-DC conversion efficiency for class-F rectifiers," *IEEE Trans. Microw. Theory Techn.*, vol. 62, no. 4, pp. 977–985, Apr. 2014.

[22] Y. Ren and K. Chang, "Bow-tie retrodirective rectenna," *Electron. Lett.*, vol. 42, no. 4, pp. 191–192, Feb. 2006.

[23] W. Tu, S. Hsu, and K. Chang, "Compact 5.8-GHz rectenna using stepped-impedance dipole antenna," *IEEE Antennas Wireless Propag. Lett.*, vol. 6, pp. 282–284, 2007.

[24] T. Kaho, R. Kishikawa, A. Miyachi, and S. Kawasaki, "Design of C-band rectifier with watt-class DC output using 0.18 μm CMOS and GaN diode," in *Proc. IEEE Wireless Power Transfer Conf.*, 2016, pp. 1–4.

[25] Y. Ohno, H. Itoh, R. Fujihara, and J. Ao, "Technologies for wireless charging in microwave cavity box using GaN Schottky barrier diode," in *Proc. IEEE Wireless Power Transfer Conf.*, 2016, pp. 1–4.